Mössbauer effect study of filled antimonide skutterudites

Gary J. Long and Dimitri Hautot
Department of Chemistry, University of Missouri–Rolla, Rolla, Missouri 65409-0010

Fernande Grandjean
Institute of Physics, B5, University of Liège, B-4000 Sart-Tilman, Belgium

Donald T. Morelli and Gregory P. Meisner
Physics and Physical Chemistry Department, General Motors Global Research and Development Operations, Warren, Michigan 48090
(Received 10 December 1998; revised manuscript received 22 February 1999)

The iron-57 Mössbauer spectra of a series of Ce-filled antimonide skutterudites, $Ce_xFe_{4-y}Co_ySb_{12}$, where x varies from 0.22 to 0.98 and y varies from 0 to 3.5, have been measured at 295 K. In addition, the spectra of $Ce_{0.60}Fe_2Co_2Sb_{12}$ and $Ce_{0.82}Fe_3CoSb_{12}$ have been measured from 85 to 295 K and the spectra of $Ce_{0.35}FeCo_3Sb_{12}$ and $Ce_{0.98}Fe_4Sb_{12}$ have been measured from 4.2 to 295 K. The spectra, all of which consist of a simple quadrupole doublet, show no evidence for any long-range magnetic ordering of any Fe magnetic moments. The 295-K quadrupole splitting increases linearly from 0.104 mm/s at $x=0.22$ to 0.415 mm/s at $x=0.98$, an increase which results from the increasing hole concentration in the valence band of these compounds. The quadrupole splitting of approximately 0.16 mm/s observed for $Ce_{0.35}FeCo_3Sb_{12}$ is virtually independent of temperature between 4.2 and 295 K and results predominantly from a lattice contribution to the electric-field gradient. In contrast, in $Ce_{0.98}Fe_4Sb_{12}$, the quadrupole splitting is constant at approximately 0.49 mm/s below approximately 70 K, and decreases with $T^{3/2}$ above 70 K. The 295-K isomer shift increases linearly from 0.345 mm/s at $x=0.22$ to 0.386 mm/s at $x=0.98$, an increase which results from a linear expansion of the unit-cell volume with increasing x. The temperature dependencies of the isomer shift and of the logarithm of the spectral absorption area in $Ce_{0.98}Fe_4Sb_{12}$ and $Ce_{0.35}FeCo_3Sb_{12}$ yield effective Mössbauer temperatures of approximately 500 and 400 K, respectively, values which are substantially higher than the Debye temperatures of approximately 300 K observed for these compounds. These differences indicate that the high-frequency vibrations of the iron sublattice are weakly coupled to the lower frequency vibrations of both the partially filled cerium sublattice and the antimony sublattice. [S0163-1829(99)00834-6]

INTRODUCTION

The high thermoelectric figure of merit recently observed[1] for the filled skutterudite compounds of formula LnM_4X_{12}, where Ln is a rare earth, M is a transition metal, and X is a pnictogen, results from a combination of a high Seebeck coefficient[2] and low thermal conductivity.[3] The band structure of these skutterudites is unusual because the highest valence band consists of hybridized transition-metal d orbitals and pnictogen p orbitals, whereas the lowest conduction band consists primarily of rare-earth f orbitals; the 0.1-eV band gap is small. The unfilled skutterudite structure,[4] which is generally given by MX_3, belongs to the body-centered-cubic space group $Im3$. The crystallographic unit cell consists of eight MX_3 units, with eight M atoms occupying the $8c$ sites and $24X$ atoms occupying the $24g$ sites of this space group. The resulting structure is characterized by nearly square rings of X atoms, a feature which represents one of the chief characteristics of the skutterudite structure.

An important feature in determining the thermoelectric properties of skutterudites is the existence of two large voids at the $2a$ positions of the unit cell, voids which are filled with additional atoms in the filled skutterudites. The rare-earth atom in the filled structure is sixfold coordinated by the X-atom planar groups and is thereby enclosed in an irregular twelvefold dodecahedral ''cage'' of X atoms. In the case of the phosphides,[5] compounds containing La, Ce, Pr, Nd, Sm, and Eu were formed. For arsenides[6] and antimonides,[7] the void volume is larger than in the phosphides and filled skutterudites can be formed with rare-earth atoms up to and including Eu, with intermediate valence Yb in $YbFe_4Sb_{12}$, and with Th in $ThOs_4As_{12}$. As noted[5] by Jeitschko and Braun, the rare-earth atom possesses an unusually large x-ray thermal parameter which is indicative of a ''rattling'' motion or participation in a soft phonon mode.

The filled skutterudites display a rich range of physical properties, which have been investigated by various methods. Mössbauer measurements[8,9] on $LaFe_4P_{12}$ indicate the presence of diamagnetic Fe, a result which is consistent with the observation of superconductivity in this compound.[10] Iron in $LaFe_4Sb_{12}$ seems to carry a magnetic moment.[11] Recent magnetic studies[12] of $CeFe_4Sb_{12}$ and $Ce_{0.9}Fe_3CoSb_{12}$ indicate that they have a Pauli susceptibility which is enhanced over that observed in the La filled and unfilled skutterudites. Additionally, it has been observed[5] that the unit-cell volume of $CeFe_4P_{12}$ is anomalously small, suggesting that there is a tendency for the Ce to attain a tetravalent or intermediate valence state, whereas only a very slight volume anomaly is observed for $CeFe_4Sb_{12}$. The tendency of Ce to be more trivalent than tetravalent in $CeFe_4Sb_{12}$ is also predicted by the band-structure calculations.[2] However, a Ce valence of 3.74 at 4.2 K was deduced[3] from electrical conductivity mea-

TABLE I. Mössbauer spectral parameters for the $Ce_xFe_{4-y}Co_ySb_{12}$ solid solutions.

Compound	T, K	δ, mm/s[a]	ΔE_Q, mm/s	Γ, mm/s	M, g/mol[b]	Θ_D, K[c]
$Ce_{0.22}Fe_{0.5}Co_{3.5}Sb_{12}$	295	0.345	0.104	0.25	-	-
$Ce_{0.35}FeCo_3Sb_{12}$	4.2	0.456	0.163	0.32	72	550
	85	0.456	0.169	0.32		
	295	0.356	0.168	0.28		
$Co_{0.47}Fe_{1.5}Co_{2.5}Sb_{12}$	295	0.358	0.252	0.27	-	-
$Ce_{0.60}Fe_2Co_2Sb_{12}$	85	0.480	0.480	0.28	72	500
	295	0.366	0.282	0.28		
$Ce_{0.71}Fe_{2.5}Co_{1.5}Sb_{12}$	295	0.375	0.335	0.25	-	-
$Ce_{0.82}Fe_3CoSb_{12}$	85	0.482	0.439	0.26	74	520
	295	0.383	0.373	0.29		
$Ce_{0.93}Fe_{3.5}Co_{0.5}Sb_{12}$	295	0.382	0.398	0.24	-	-
$Ce_{0.98}Fe_4Sb_{12}$	4.2	0.491	0.516	0.24	69	520
	85	0.487	0.505	0.26		
	295	0.386	0.415	0.28		
$LaFe_4Sb_{12}$	295	0.391	0.382	0.24	-	-

[a]The isomer shifts are reported relative to room-temperature α-iron foil.

[b]Obtained by using only the higher temperature data points; see text.

[c]Obtained by using the M values given and the complete temperature dependence of the isomer shift; see text.

surements. Iron-57 Mössbauer measurements[13] on $YbFe_4Sb_{12}$ indicate that Fe carries no magnetic moment and x-ray appearance near-edge structure (XANES) measurements[13] at the Yb L_{III} edge reveal an intermediate valence state for Yb. Obviously the question of the iron and the rare-earth valence states[2,3,13,14] has important consequences in determining whether these filled skutterudites are metallic, semiconducting, or even superconducting, magnetic, or nonmagnetic.

In order to investigate the electronic and dynamic properties of the Fe atoms in filled skutterudites, we have undertaken a Mössbauer spectral study of the $Ce_xFe_{4-y}Co_ySb_{12}$ solid solutions. Previous studies[14,15] on these compounds have shown that the amount of Ce, x, filling the voids is a strong function of the Fe/Co ratio; for $y=0$, nearly all the voids can be filled, i.e., x is nearly one, whereas for $y=4$, only about 10% of the voids can be filled. It has also been shown[16] that the lattice thermal conductivity and structural properties of these fractionally filled skutterudites can best be rationalized if they are considered to be solid solutions of fully filled $CeFe_4Sb_{12}$ and $\square Co_4Sb_{12}$, where $\square$ is the unoccupied rare-earth site in $CoSb_3$, such that the general stoichiometric formula is $(CeFe_4Sb_{12})_{1-\alpha}(\square Co_4Sb_{12})_\alpha$, and in the corresponding general formula, $Ce_xFe_{4-y}Co_ySb_{12}$, x is $1-\alpha$ and y is 4α.

EXPERIMENT

Samples of $Ce_xFe_{4-y}Co_ySb_{12}$ were prepared as described previously[15] and were the same samples as were used in the lattice thermal-conductivity study.[16] The Mössbauer spectra were obtained between 4.2 and 295 K on a constant-acceleration spectrometer which utilized a room-temperature rhodium matrix cobalt-57 source and was calibrated at room temperature with α-iron foil. The absorber thicknesses ranged from 35 mg/cm^2 for $Ce_{0.98}Fe_4Sb_{12}$ to 39 mg/cm^2 for $Ce_{0.22}Fe_{0.5}Co_{3.5}Sb_{12}$. The resulting spectra have been fit as discussed below and the estimated absolute errors are ± 0.005 mm/s for the isomer shifts, and ± 0.01 mm/s for the quadrupole splittings and linewidths. The isomer shifts are reproducible to ± 0.0025 mm/s, the quadrupole splittings are reproducible to ± 0.005 mm/s, and the absolute spectral absorption areas are reproducible to $\pm 0.5\%$ of the area expressed as (% effect)(mm/s).

RESULTS AND DISCUSSION

The Mössbauer spectra have been measured between 4.2 and 295 K for $Ce_{0.35}FeCo_3Sb_{12}$ and $Ce_{0.98}Fe_4Sb_{12}$, between 85 and 295 K for $Ce_{0.60}Fe_2Co_2Sb_{12}$ and $Ce_{0.82}Fe_3CoSb_{12}$, and at 295 K for the remaining samples. A summary of the Mössbauer spectral parameters is given in Table I and some typical spectra, obtained at 85 K, are shown in Fig. 1. All the observed spectra are quadrupole doublets which have been fit with two lines of equal linewidths between 0.24 and 0.32 mm/s and essentially equivalent areas.

The reported[17] hyperfine parameters for $FeSb_2$ are quite different from those presented in Table I and there is no indication in the spectra for the presence of $FeSb_2$ in any of these compounds. Further, in no case was there any indication of magnetic ordering in any of the Mössbauer spectra, even at 4.2 K. Thus the Fe atoms in these compounds carry no magnetic moment and the magnetic behavior of $CeFe_4Sb_{12}$ cannot be attributed[18] to the magnetism of the $[Fe_4Sb_{12}]^{3-}$ polyanion. It is likely that the intermediate valence[2,3,14] Ce carries a magnetic moment just as intermediate valence[13] Yb carries a moment in $YbFe_4Sb_{12}$.

In understanding the various trends in the spectral hyperfine parameters it is very useful to consider the Fe Wigner-Seitz cell and its volume, which provide a well defined picture of the Fe near-neighbor environment. Thus we have calculated[19] the Wigner-Seitz cells for $FeSb_3$, $CoSb_3$, $CeFe_4Sb_{12}$, and $LaFe_4Sb_{12}$ by using the previously reported structural parameters[7,20,21] and the 12-coordinate metallic ra-

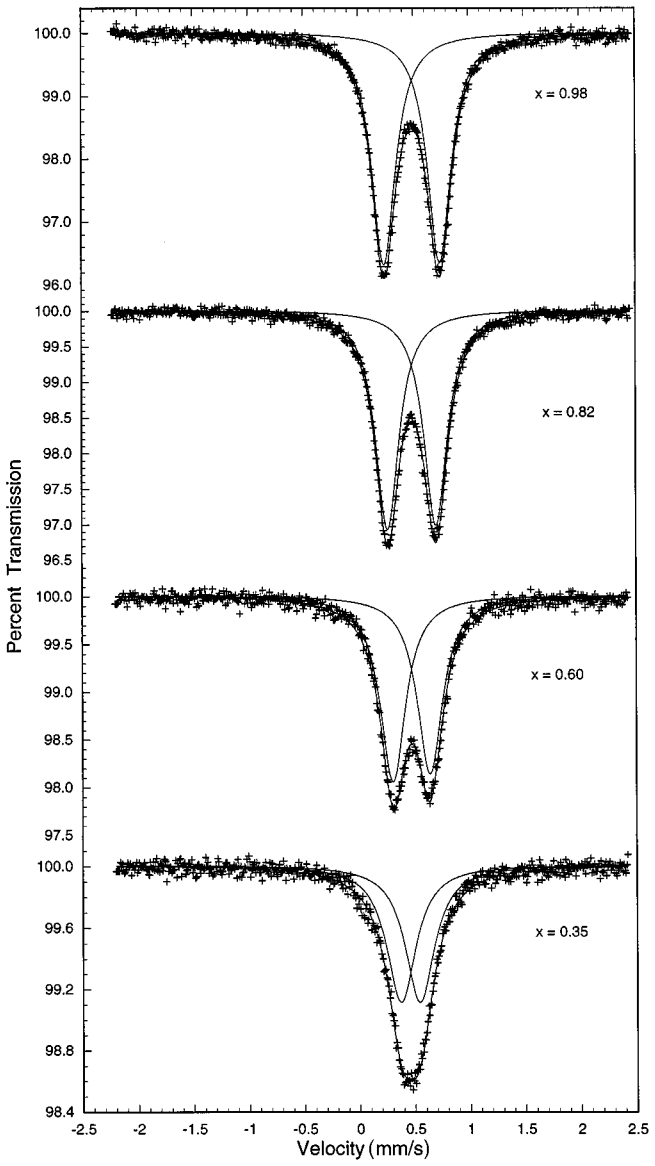

FIG. 1. The Mössbauer-effect spectra of several of the $Ce_xFe_{4-y}Co_ySb_{12}$ solid solutions measured at 85 K.

dii of 1.28 Å for P, 1.26 Å for Fe, 1.25 Å for Co, 1.59 Å for Sb, 1.87 Å for La, and 1.81 Å for Ce. The results of these calculations are given in Table II.

When interpreting the various Mössbauer spectral hyperfine parameters it is important to realize that the materials under study can be considered either as having a random distribution of Ce and Fe throughout the lattice or a nonrandom association of Fe with Ce, but only on an immediate near-neighbor distance scale. In the former case there would be a variation in the structural environment about an Fe site that could, at least in part, account for variations in the hyperfine parameters. In the latter case the various compounds can be considered as solid solutions[16] of fully filled $CeFe_4Sb_{12}$ and $\square Co_4Sb_{12}$, with the general formula $(CeFe_4Sb_{12})_{1-\alpha}(\square Co_4Sb_{12})_\alpha$, where $\square$ represents a vacancy. Hence there would be relatively little change in the structural environment about an Fe site with x and the observed changes in the hyperfine parameters would have to be predominantly electronic in nature. As will be demonstrated below, we believe the latter case predominates.

Linewidth. As is evident in Table II, the Fe $8c$ site in these compounds has only Sb $24g$ sites as near neighbors and, more specifically, it does not have another Fe or Co $8c$ site as a near neighbor. Thus the replacement of Fe by Co on the $8c$ site yields little change in the near-neighbor environment about the Fe $8c$ probe atom and, indeed, there is no evidence for the broadening of the Mössbauer spectral linewidth with increasing amounts of Co; see Table I. If Ce is randomly but uniformly distributed throughout the lattice then the Fe $8c$ site may have either zero, one, or two Ce near neighbors. However, the narrow observed Mössbauer spectral linewidths do not reflect this possibility and hence support the presence of the $(CeFe_4Sb_{12})_{1-\alpha}(\square Co_4Sb_{12})_\alpha$ solid solutions.[16]

Quadrupole interaction. The quadrupole interaction, which for iron-57 is identical to the quadrupole splitting ΔE_Q, is related to the electric-field gradient eq at an iron-57 nucleus by the relationship $\Delta E_Q=(1/2)e^2qQ(1+\eta^2/3)^{1/2}$, where Q is the iron-57 nuclear quadrupole moment and η is the asymmetry parameter. The virtually linear increase of ΔE_Q with x in $Ce_xFe_{4-y}Co_ySb_{12}$ and the close to linear increase of ΔE_Q with the increasing number of holes per formula unit[14] are illustrated in Fig. 2.

The electric-field gradient eq at a site in a noncubic metallic lattice arises[22] from two independent contributions, the lattice contribution eq^{latt} and the nonspherical conduction-electron distribution contribution eq^{ce} and is given by

$$eq=(1-\gamma)\sum eq^{\text{latt}}+(1-R)\sum eq^{\text{ce}}, \qquad (1)$$

where the Sternheimer antishielding factors $(1-\gamma)$ and $(1-R)$ describe the amplification of each contribution by the closed electron shells of the probe atom.

In order to determine the relative importance of the two contributions to the electric-field gradient described in Eq. (1), we have used the positions of the six near-neighbor Sb atoms, with an assumed charge of $+3$, to calculate, with the point-charge approximation, the expected lattice contribution to the electric-field gradient at the Fe site in $CeFe_4Sb_{12}$. It is always difficult to assign charge states to atoms in intermetallic compounds and, in this case, we have used $+3$ for Sb because it is consistent with the observed[20] Mössbauer spectra of $CoSb_3$ and because this value yields an upper bound value of 0.08 mm/s for the Sb contribution, a value which is expected to be virtually independent of temperature and x. The only additional lattice contribution would result from the presence of two near-neighbor Ce atoms at a distance of 3.956 Å, atoms that are found to be formal Wigner-Seitz near neighbors to Fe, see Table II, but to comprise only a very small portion of the surface area of the Wigner-Seitz cell. Then, if we assume a Ce charge of $+3.74$, as calculated from the carrier concentration,[15] a point-charge calculation yields an additional lattice contribution of at most 0.08 mm/s. Because the Sb and Ce ions are on a crystallographic threefold axis, the asymmetry parameter η is zero. The resulting sum of 0.16 mm/s actually represents the upper bound for the lattice contribution because of the Sternheimer antishielding process, the approximate charges used, and the assumption of two Ce near neighbors. Of course, at $x=0$ no

TABLE II. Near-neighbor environments, Wigner-Seitz cell volumes, and unit-cell volumes.

		Number of W-S near neighbors					
Compound	Site	*Ln*, 2*a*	Co or Fe, 8*c*	Sb or P, 24*g*	V_{WS}, Å^3	$V_{unit\ cell}$, Å^3	Ref.
$CoSb_3$	Co, 8*c*	-	0	6	9.87	737.5	25
	Sb, 24*g*	-	2	10	27.44		
$FeSb_3$	Fe, 8*c*	-	0	6	10.89	772.7	26
	Sb, 24*g*	-	2	10	28.56		
$CeFe_4Sb_{12}$	Ce, 2*a*	0	(8)[a]	12	33.41	762.3	7
	Fe, 8*c*	(2)[a]	0	6	10.52		
	Sb, 24*g*	1	2	10	25.47		
$LaFe_4Sb_{12}$	La, 2*a*	0	(8)[b]	12	35.26	763.4	7
	Fe, 8*c*	(2)[b]	0	6	10.52		
	Sb, 24*g*	1	2	10	25.36		
$LaFe_4P_{12}$	La, 2*a*	0	(8)[c]	12	32.50	480.3	5
	Fe, 8*c*	(2)[c]	0	6	10.85		
	P, 24*g*	1	2	10	13.69		
$CeFe_4P_{12}$	Ce, 2*a*	0	(8)[d]	12	30.31	473.1	5
	Fe, 8*c*	(2)[d]	0	6	10.75		
	P, 24*g*	1	2	10	13.60		

[a]These Wigner-Seitz cell defined near neighbors are at 3.956 Å and comprise only 3.0 and 1.7% of the surface areas of the Ce, 2*a* and Fe, 8*c* cells, respectively.

[b]These Wigner-Seitz cell defined near neighbors are at 3.958 Å and comprise only 2.9 and 1.6% of the surface areas of the La, 2*a* and Fe, 8*c* cells, respectively.

[c]These Wigner-Seitz cell defined near neighbors are at 3.391 Å and comprise 18.6 and 8.6% of the surface areas of the La, 2*a* and Fe, 8*c* cells, respectively.

[d]These Wigner-Seitz cell defined near neighbors are at 3.374 Å and comprise 17.9 and 8.0% of the surface areas of the Ce, 2*a* and Fe, 8*c* cells, respectively.

Ce would be present, and the upper bound would be 0.08 mm/s, which would be the hypothetical quadrupole splitting observed if $CoSb_3$ contained a trace of iron-57. This estimation also assumes that the distortion of the Sb octahedron about Fe is identical in $CeFe_4Sb_{12}$ and in $CoSb_3$. Actually, the Sb octahedron is less distorted[7] in $CoSb_3$ and hence the quadrupole splitting in $CoSb_3$ is expected to be even smaller than 0.08 mm/s. This estimation compares well with the quadrupole splitting of 0.104 mm/s measured in $Ce_{0.22}Fe_{0.5}Co_{3.5}Sb_{12}$; see Table I. Thus the maximum expected lattice contribution to the quadrupole splitting, which has been shown as the dashed line in Fig. 2, is much smaller than the 0.415-mm/s value observed at 295 K for $Ce_{0.98}Fe_4Sb_{12}$. Hence we must conclude that the conduction-electron contribution to the quadrupole splitting amounts to at least approximately 0.25 mm/s and could be as much as approximately 0.6 mm/s if the two terms in Eq. (1) have different signs.

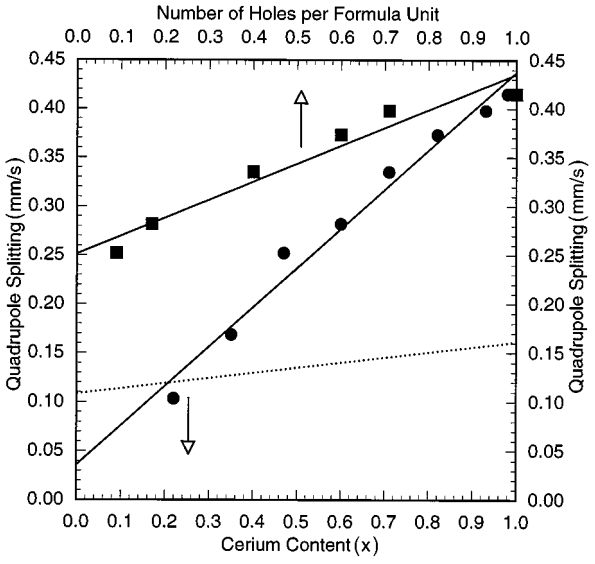

FIG. 2. The variation with Ce content *x*, ●, and with the number of holes per formula unit, ■, of the 295-K quadrupole splitting observed in $Ce_xFe_{4-y}Co_ySb_{12}$. The dashed line represents a point-charge calculation of the lattice contribution to the quadrupole splitting as is discussed in the text. The error bars are essentially the size of the data points.

It is tempting to associate the changes observed in Fig. 2 with structural changes about Fe. However, whether the compounds are $Ce_xFe_{4-y}Co_ySb_{12}$, with a random distribution of Fe and Co, or are $(CeFe_4Sb_{12})_{1-\alpha}(\square Co_4Sb_{12})_\alpha$ solid solutions, the Fe atom has the same near-neighbor environment of Sb and Ce. Hence the changes in the quadrupole splitting with *x* cannot be explained by the presence of Co atoms which are next nearest rather than nearest neighbors of Fe. Thus we conclude that the increase in quadrupole splitting results from an increasing concentration of holes in the valence band[15,16] in these *p*-type semiconducting materials, as is shown in Fig. 2.

The temperature dependence of the quadrupole splitting for four of the compounds is shown in Fig. 3. The temperature dependence of the electric-field gradient in a noncubic

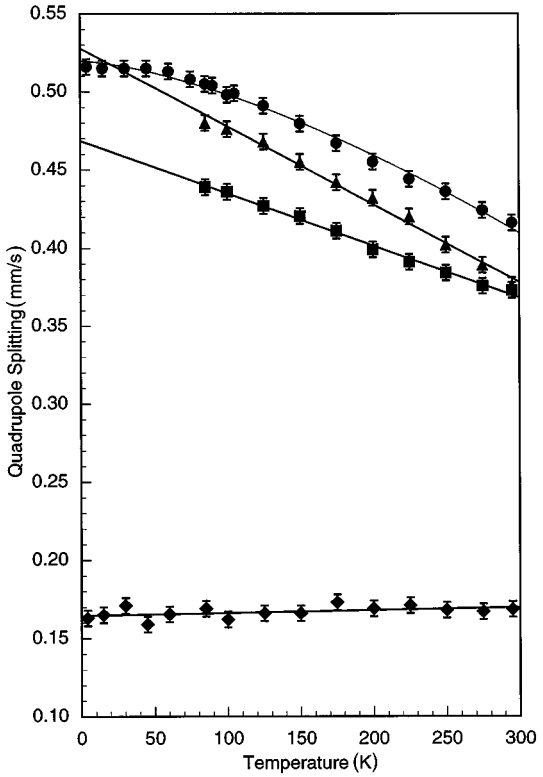

FIG. 3. The temperature dependence of the quadrupole splittings observed in $Ce_{0.35}FeCo_3Sb_{12}$, ♦, $Ce_{0.60}Fe_2Co_2Sb_{12}$, ▲, $Ce_{0.82}Fe_3CoSb_{12}$, ■, and $Ce_{0.98}Fe_4Sb_{12}$, ●. The $Ce_{0.98}Fe_4Sb_{12}$ results have been fit with Eq. (3), see text.

metallic lattice has been fit[23] with different functions. The first relationship, the ''$T^{3/2}$ law,'' is given by

$$eq = eq(0)(1-\beta T^{3/2}), \tag{2}$$

where $eq(0)$ is the electric-field gradient at absolute zero temperature. The β parameter has been found[22] to vary between 1×10^{-5} and $7\times10^{-5}\,\mathrm{K}^{-3/2}$. The second relationship, the ''T^{γ} law,'' is given by

$$eq = eq(0)(1-\beta T^{\gamma}), \tag{3}$$

where γ was found to have values of approximately 1.4 with a standard deviation of 0.4. The third relationship, the quadratic law, is given by

$$eq = eq(0)(1+BT+CT^2). \tag{4}$$

We have fit the temperature dependence of the quadrupole splitting in $Ce_{0.98}Fe_4Sb_{12}$, shown in Fig. 3 with Eqs. (2)–(4), and find that the first two equations give equally good fits with $\Delta E_Q(0)=0.52\,\mathrm{mm\,s}$, $\beta=4.3\times10^{-5}\,\mathrm{K}^{-3/2}$, and $\gamma=1.49$. The fit with Eq. (3) is shown in Fig. 3 and is slightly better than the fit with the quadratic law, Eq. (4). The value of γ indicates that the ''$T^{3/2}$'' law is adequate and the value of β is in the expected range.

Chen *et al.*[14] have measured the hole concentration in $Ce_{0.98}Fe_4Sb_{12}$ and found that it was virtually constant at $1\times10^{21}\,\mathrm{cm}^{-3}$ between 2 and approximately 70 K. Above 70 K the hole concentration increases with an approximately $T^{3/2}$ dependence. In a parallel fashion, the quadrupole splitting is found to be independent of temperature from 4.2 to approximately 70 K and then to decrease with approximately a $T^{3/2}$ dependence. Up to now, there is no theoretical understanding[23] of the $T^{3/2}$ dependence of the quadrupole splitting in metallic hosts. It is generally believed that the thermal vibrations of the lattice are responsible for this temperature dependence. We believe that the decrease in the quadrupole splitting above approximately 70 K is due to a combined effect of the thermal lattice vibrations, the thermal lattice expansion, the increase in hole concentration,[15,16] and the decrease in hole mobility[24] with increasing temperature.

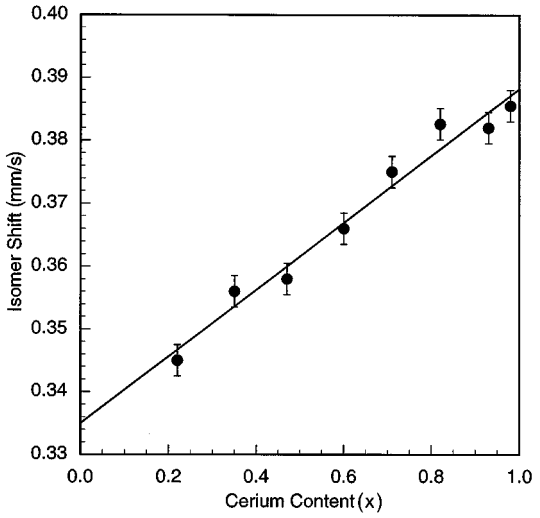

FIG. 4. The variation with Ce content x of the 295-K isomer shifts observed in $Ce_xFe_{4-y}Co_ySb_{12}$.

More recent studies[24] indicate that the hole concentration decreases with decreasing x from a value of approximately $3\times10^{21}\,\mathrm{cm}^{-3}$ at higher values of x down to values of approximately $1\times10^{19}\,\mathrm{cm}^{-3}$ at low values of x in the $Ce_xFe_{4-y}Co_ySb_{12}$ solid solutions. This decrease agrees with the decrease in the quadrupole splitting which approaches the calculated maximum lattice contribution at x values of 0.35 and 0.22.

Isomer shift. There is a linear increase in the isomer shift measured at 295 K both with x, as is shown in Fig. 4, and with unit-cell volume. Thus, as the unit-cell volume or hole concentration increases, there is a decrease in s-electron density at the iron-57 nucleus in the $Ce_xFe_{4-y}Co_ySb_{12}$ solid solutions. Apparently, the presence of the holes, in conjunction with the expanding unit cell, permits the expansion of the $4s$ electron radial distribution function, thus decreasing the s-electron density at the nucleus and increasing the isomer shift. The volume dependence of the isomer shift, expressed[25] as $\Delta\delta/\Delta\ln V$, is 1.42 mm/s, a value which agrees well with the value of 1.31 mm/s observed[25] for α-iron. Hence it seems that the x dependence of the isomer shift is well understood in terms of the unit-cell expansion.

The isomer shifts of $LaFe_4Sb_{12}$, given in Table I, and of $YbFe_4Sb_{12}$,[13] are very similar to that of $Ce_{0.98}Fe_4Sb_{12}$, indicating rather similar s-electron density at Fe in these compounds. In contrast, these isomer shifts are much larger than the 0.050 mm/s value observed[8] for $LaFe_4P_{12}$, although it should be noted that the temperature dependence of the isomer shift of $Ce_{0.98}Fe_4Sb_{12}$, see below, and $LaFe_4P_{12}$ are quite similar. The temperature dependence of the isomer shift in

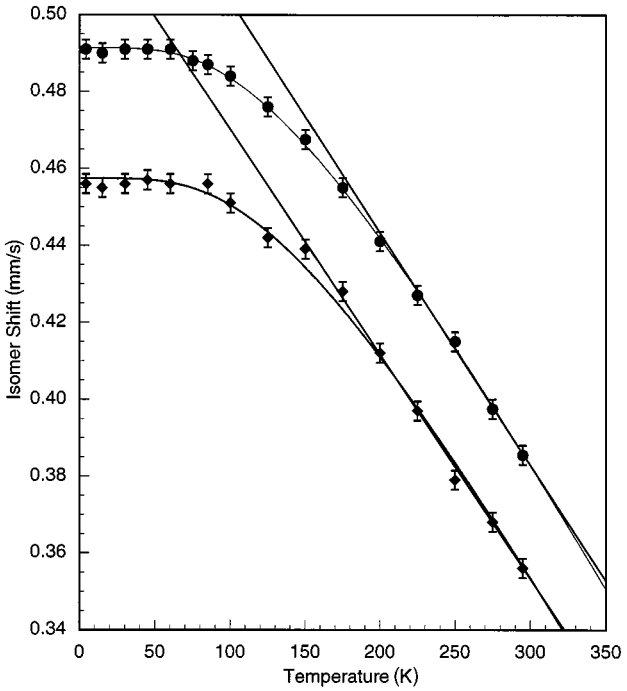

FIG. 5. The temperature dependence of the isomer shifts observed in $Ce_{0.35}FeCo_3Sb_{12}$, ♦, and $Ce_{0.98}Fe_4Sb_{12}$, ●.

$Ce_{0.98}Fe_4Sb_{12}$ and $Ce_{0.35}FeCo_3Sb_{12}$ is shown in Fig. 5. The results for $Ce_{0.82}Fe_3CoSb_{12}$ and $Ce_{0.60}Fe_2Co_2Sb_{12}$ are very similar and would appear between the two curves shown in Fig. 5.

Because the lattice properties of the $Ce_xFe_{4-y}Co_ySb_{12}$ solid solutions are very important for their potential applications, we have undertaken a detailed analysis of the temperature dependence of the isomer shift in terms of the Debye model for the second-order Doppler shift. It is well known that the Debye model is strictly applicable to only a unielemental lattice. However, the concept of the Debye temperature is commonly used[8,12,26] to describe complex lattices such as the skutterudite lattice. In this model, the temperature dependence of the isomer shift δ is given by

$$\delta = \delta_0 - \frac{\langle \nu^2 \rangle}{2c}, \tag{5}$$

where δ_0 is the isomer shift at absolute zero temperature and

$$\langle \nu^2 \rangle = \frac{9k\theta_D}{8M} + \frac{3kT}{M} f\left(\frac{T}{\theta_D}\right), \tag{6}$$

where

$$f\left(\frac{T}{\theta_D}\right) = 3\left(\frac{T}{\theta_D}\right)^3 \int_0^{\theta_D/T} \frac{x^3 dx}{e^x - 1}. \tag{7}$$

In these expressions, $\langle \nu^2 \rangle$ is the mean-square velocity of the iron-57 nuclide, k is the Boltzmann constant, c is the velocity of light, M is the effective recoil mass, and θ_D is the Debye temperature. At temperatures well below the Debye temperature, $\langle \nu^2 \rangle$ is given by

$$\langle \nu^2 \rangle = \frac{9k\theta_D}{8M} + \frac{3\pi^4 kT}{5M}\left(\frac{T}{\theta_D}\right)^3 \tag{8}$$

and thus the isomer shift will become constant at low temperature. In contrast at temperatures well above the Debye temperature $\langle \nu^2 \rangle$ is given by

$$\langle \nu^2 \rangle = \frac{3kT}{M}\left\{1 + \frac{1}{20}\left(\frac{\theta_D}{T}\right)^2 - \frac{1}{1680}\left(\frac{\theta_D}{T}\right)^4 + \cdots\right\} \tag{9}$$

and, to a first approximation, the isomer shift will be a function of the effective recoil mass M and will decrease linearly with increasing temperature. In the analysis of the temperature dependence of the Mössbauer-effect isomer shift, it is often found that the recoil mass takes on values above 57 g/mol, the mass of the iron-57 Mössbauer nuclide. This occurs because the effective mass of the recoiling nuclide is increased through covalent bonding with its near neighbors. In the discussion that follows the Debye temperature will be referred to as the effective Mössbauer temperature when the effective recoil mass is not 57 g/mol.

The value of the effective masses in the $Ce_xFe_{4-y}Co_ySb_{12}$ solid solutions has been determined from a linear fit to the higher temperature data points, as is shown in Fig. 5. The resulting values, given in Table I, range from 69–74 g/mol but are all effectively the same as their estimated accuracy is at best ±4 g/mol. A similar value of approximately 70 g/mol for all the compounds is not surprising, especially if the environment about Fe is really quite similar as expected[16] in the $(CeFe_4Sb_{12})_{1-\alpha}(\square Co_4Sb_{12})_\alpha$ solid solutions. However, approximately 70 g/mol is substantially higher than the 57 g/mol value expected for iron-57 in the absence of covalency. The presence of substantial covalency in the Fe-Sb bonding is not unexpected because the observed Fe-Sb bond distance of 2.56 Å is substantially smaller than either the 2.85-Å sum of the metallic radii or the 2.68-Å sum of the covalent radii for these two elements. Further, antimony-121 Mössbauer spectral studies[20] indicate the presence of substantial covalency in $CoSb_3$ and related compounds.

The fit of the complete temperature dependence of the isomer shifts in $Ce_{0.98}Fe_4Sb_{12}$ and $Ce_{0.35}FeCo_3Sb_{12}$ is also shown in Fig. 5. Unfortunately, as is shown in Fig. 6 for $Ce_{0.98}Fe_4Sb_{12}$, there is a very strong correlation between the effective recoil mass and the Debye or effective Mössbauer temperature. A very similar contour plot is obtained for $Ce_{0.35}FeCo_3Sb_{12}$. In the plot shown in Fig. 6, any combination of values within the inner contour will reproduce the temperature dependence of the isomer shifts to within their experimental accuracy. It should be noted that the value of 69 g/mol, obtained from the higher temperature values, does not fall within this contour. This occurs because the higher temperatures are not sufficiently above the Debye temperature to allow the approximation to work well.

A careful inspection of Fig. 6 reveals that, for $Ce_{0.98}Fe_4Sb_{12}$, the effective iron-57 recoil mass can range from 57–65 g/mol and the corresponding effective Debye or Mössbauer temperatures can range from 540–440 K. For $Ce_{0.35}FeCo_3Sb_{12}$ a similar contour plot indicates that the effective recoil mass can range from 57–65 g/mol and the corresponding effective Mössbauer temperatures can range from 560–460 K. Thus it appears that these values are es-

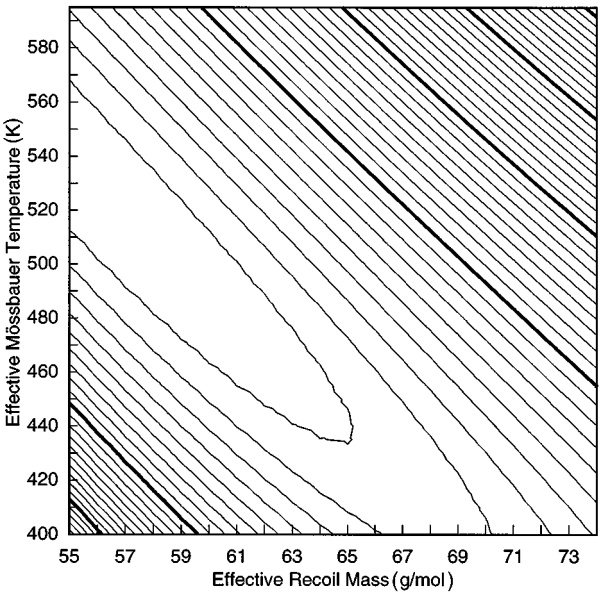

FIG. 6. A contour plot of the values of the effective recoil mass and the effective Debye or Mössbauer temperature which are consistent with the isomer shifts observed in $Ce_{0.98}Fe_4Sb_{12}$. Any pair of values found within the inner contour will fit the experimental isomer shifts within the experimental errors. Each major and minor contour corresponds, respectively, to a 0.0005 and a 0.00005 increase in the sum of squares misfit.

sentially independent of Ce content, a conclusion that is consistent with the formulation[16] of these solid solutions as $(CeFe_4Sb_{12})_{1-\alpha}(\square Co_4Sb_{12})_\alpha$. For comparison, it should be noted that a Debye temperature of 450 K was obtained[8] for

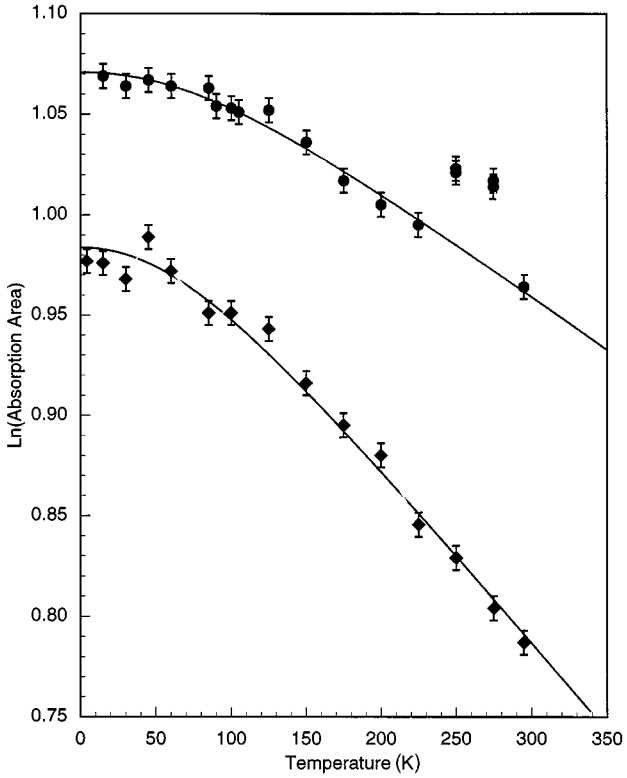

FIG. 7. The temperature dependence of the logarithm of the Mössbauer spectral absorption areas observed for $Ce_{0.35}FeCo_3Sb_{12}$, ♦, and $Ce_{0.98}Fe_4Sb_{12}$, ●.

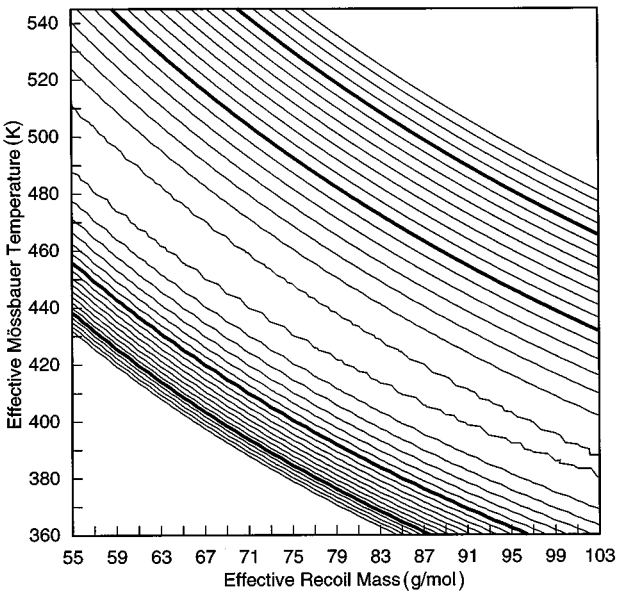

FIG. 8. A contour plot of the values of the effective recoil mass and the effective Mössbauer temperature which are consistent with the Mössbauer spectral absorption areas observed in $Ce_{0.98}Fe_4Sb_{12}$. Any pair of values found within the inner contour will fit the experimental values within the experimental errors. Each major and minor contour corresponds, respectively, to a 0.001 and a 0.00015 increase in the sum of squares misfit.

$LaFe_4P_{12}$ from the temperature dependence of the isomer shift.

Mössbauer spectral absorption area. The Mössbauer spectral absorption area is proportional to the iron-57 recoil free factor f which is related to the Debye or effective Mössbauer temperature by

$$f=\exp\left\{-\frac{3}{4}\frac{E_\gamma^2}{Mc^2k\theta_D}\left[1+4\left(\frac{T}{\theta_D}\right)^2\int_0^{\theta_D/T}\frac{x\,dx}{\exp x-1}\right]\right\}. \tag{10}$$

This expression has been used to fit the Mössbauer spectral absorption areas and the results are shown for $Ce_{0.98}Fe_4Sb_{12}$ and $Ce_{0.35}FeCo_3Sb_{12}$ in Fig. 7. Once again, as indicated by the contour plot shown in Fig. 8, there is a very strong correlation between the effective recoil mass and the effective Mössbauer temperature. If one accepts the limits placed on the effective recoil mass by the isomer shift, see above, then these results indicate that the effective Mössbauer temperature can range from 460–560 K for $Ce_{0.98}Fe_4Sb_{12}$ and from 350–420 K for $Ce_{0.35}FeCo_3Sb_{12}$. It should be noted in Fig. 7 that the absorption area for $Ce_{0.98}Fe_4Sb_{12}$ at 250 and 275 K is larger than expected based on the data at the remaining temperatures. A similar, but smaller, increase has also been observed at these temperatures in $Ce_{0.82}Fe_3CoSb_{12}$, but not in $Ce_{0.60}Fe_2Co_2Sb_{12}$ and $Ce_{0.35}FeCo_3Sb_{12}$. This ''anomaly'' is reproducible within the expected error limits as determined by repeated measurements on a given sample. The reason of this ''anomaly'' is not apparent at this time.

Because an in-depth understanding of the lattice vibrational properties of the skutterudites is important in understanding their thermoelectric properties, it is worthwhile to

discuss the values of the Debye temperature obtained from different techniques and calculations. Recent low-temperature specific-heat measurements[12] on $CeFe_4Sb_{12}$ and $Ce_{0.9}Fe_3CoSb_{12}$ have yielded Debye temperatures of 250 and 257 K, respectively. Debye temperatures of approximately 300 K have been observed[26] in $LaFe_4Sb_{12}$ and $La_{0.75}Fe_3CoSb_{12}$. These values, which describe the vibrational properties of the three kinds of atoms in the structure, are substantially lower than the Mössbauer spectral based values which describe the vibrational properties of the iron atoms in the structure. Indeed different vibrational frequencies are probed by different techniques. For instance, Raman scattering spectra[27] probe the Sb vibrations in the lattice, whereas infrared spectra[28] probe the Fe vibrations. The Sb vibrational frequencies are lower[29,30] than the Fe vibrational frequencies, a difference which is in agreement with the high effective Mössbauer temperatures observed herein. The vibrational frequencies of the rare-earth atom responsible for the good thermal properties of the skutterudites are found at approximately 200 cm^{-1} and these modes are coupled to the Sb vibrational modes. The Mössbauer spectral measurements confirm that the Fe vibrational modes are weakly coupled to the rare-earth and Sb vibrational modes. Indeed, the effective Mössbauer temperature of approximately 450 K obtained herein is only slightly different from the Debye temperature[31] of α-iron of 480 ± 5 K obtained from the temperature dependencies of the Mössbauer spectral isomer shifts and absorption areas. Hence it would be very interesting to study the Eu-151 Mössbauer spectra of Eu filled and partially filled skutterudites in order to investigate directly the vibrational properties of the Eu atom.

CONCLUSIONS

The iron-57 Mössbauer spectra of the $Ce_xFe_{4-y}Co_ySb_{12}$ solid solutions provide substantial insight into the electronic structure and lattice dynamics of these materials from the point of view of the Fe sublattice. First, they reveal no long range magnetic ordering involving Fe. They confirm the $(CeFe_4Sb_{12})_{1-\alpha}(\square Co_4Sb_{12})_\alpha$ solid solution nature of these compounds[16] by the lack of any spectral broadening with decreasing x, or increasing α, by the linear dependence of the observed quadrupole splitting upon x, by the temperature dependence of the quadrupole splitting, and by the virtual independence of the effective Mössbauer temperature upon x. The quadrupole splitting is close to linearly related to the hole concentration and is dominated by the electronic contribution. The changes in the isomer shift with x and with temperature may be accounted for by changes in the unit-cell volume and the Wigner-Seitz cell volume available to Fe. The temperature dependence of the isomer shift and the spectral absorption area yields values for the effective Mössbauer temperature which are higher than those obtained from specific-heat studies and are essentially independent of x. Hence the phonon modes related to the Fe and Co sublattice are relatively independent of the presence of the rattling Ce present in these filled and partially filled skutterudites.

ACKNOWLEDGMENTS

We would like to thank Dr. A. Hautot for helpful discussions during the course of this work and B. Little for experimental help in obtaining the spectra. This research was supported in part by the U.S. National Science Foundation through a Division of Materials Research, Grant No. 95-21739.

[1] B. C. Sales, D. Mandrus, and R. K. Williams, Science **272**, 1325 (1996); J.-P. Fleurial, A. Borshchevsky, T. Caillat, D. T. Morelli, and G. P. Meisner, in *Proceedings of the 15th International Conference on Thermoelectrics*, Pasadena, CA, 1996, edited by T. Caillat (Institute for Electrical and Electronics Engineers, Piscataway, NJ, 1996), p. 91.

[2] L. Nordström and D. J. Singh, Phys. Rev. B **53**, 1103 (1996); H. Anno, K. Hatada, H. Shimizu, K. Matsubara, Y. Notohara, T. Sakakibara, H. Tashiro, and K. Motoya, J. Appl. Phys. **83**, 5270 (1998).

[3] D. T. Morelli and G. P. Meisner, J. Appl. Phys. **77**, 3777 (1995).

[4] I. Oftedal, Z. Kristallogr. **66**, 517 (1928).

[5] W. Jeitschko and D. Braun, Acta Crystallogr., Sect. B: Struct. Crystallogr. Cryst. Chem. **B33**, 3401 (1977).

[6] D. J. Braun and W. Jeitschko, J. Solid State Chem. **32**, 357 (1980).

[7] D. J. Braun and W. Jeitschko, J. Less-Common Met. **72**, 147 (1980); B. H. Evers, W. Jeitschko, L. Boonk, D. J. Braun, T. Ebel, and U. D. Scholz, J. Alloys Compd. **224**, 184 (1995); N. R. Dilley, E. J. Freeman, E. D. Bauer, and M. B. Maple, Phys. Rev. B **58**, 6287 (1998).

[8] G. K. Shenoy, D. R. Noakes, and G. P. Meisner, J. Appl. Phys. **53**, 2628 (1982).

[9] F. Grandjean, A. Gérard, D. J. Braun, and W. Jeitschko, J. Phys. Chem. Solids **45**, 877 (1984).

[10] G. P. Meisner, Physica B&C **108B**, 763 (1981).

[11] B. C. Sales, D. Mandrus, B. C. Chakoumakos, V. Keppens, and J. R. Thompson, Phys. Rev. B **56**, 15 018 (1997).

[12] D. A. Gajewski, N. R. Dilley, E. D. Bauer, E. J. Freeman, R. Chau, M. B. Maple, D. Mandrus, B. C. Sales, and A. H. Lacerda, J. Phys.: Condens. Matter **10**, 6973 (1998).

[13] A. Leithe-Jasper, D. Kaczorowski, P. Rogl, J. Bogner, M. Reissner, W. Steiner, G. Wiesinger, and C. Godart, Solid State Commun. **109**, 395 (1999).

[14] B. Chen, J.-H. Xu, C. Uher, D. T. Morelli, G. P. Meisner, J.-P. Fleurial, T. Caillat, and A. Borshchevsky, Phys. Rev. B **55**, 1476 (1997).

[15] D. T. Morelli, G. P. Meisner, B. Chen, S. Hu, and C. Uher, Phys. Rev. B **56**, 7376 (1997).

[16] G. P. Meisner, D. T. Morelli, S. Hu, J. Yang, and C. Uher, Phys. Rev. Lett. **80**, 3551 (1998).

[17] A. Gérard, Colloq. Int. C. N. R. S. **157**, 55 (1967); J. Steger and E. Kostiner, J. Solid State Chem. **5**, 131 (1972).

[18] M. E. Danebrock, C. B. H. Evers, and W. Jeitschko, J. Phys. Chem. Solids **57**, 381 (1996).

[19] L. Gelato, J. Appl. Crystallogr. **14**, 141 (1980).

[20] A. Kjekshus and T. Rakke, Acta Chem. Scand. **A28**, 99 (1974); A. Kjekshus, D. G. Nicholson, and T. Rakke, Acta Chem. Scand. **27**, 1315 (1973).

[21] M. D. Hornbostel, E. J. Hyer, J. Thiel, and D. C. Johnson, J. Am. Chem. Soc. **119**, 2665 (1997).
[22] R. Vianden, Hyperfine Interact. **16**, 189 (1983).
[23] H. C. Varma and G. N. Rao, Hyperfine Interact. **16**, 207 (1983).
[24] D. Morelli (unpublished).
[25] D. L. Williamson, in *Mössbauer Isomer Shifts*, edited by G. K. Shenoy and F. E. Wagner (North-Holland, Amsterdam, 1978), p. 317.
[26] B. C. Sales, D. Mandrus, B. C. Chakoumakos, and J. W. Sharp, Bull. Am. Phys. Soc. **44**, 428 (1999), paper IC23 5.
[27] G. S. Nolas and C. A. Kendziora, Phys. Rev. B **59**, 6189 (1999).
[28] H. D. Lutz and G. Kliche, Z. Anorg. Allg. Chem. **480**, 105 (1981).
[29] M. Fornari and D. J. Singh, Bull. Am. Phys. Soc. **44**, 428 (1999), paper IC23 3.
[30] M. Fornari and D. J. Singh, J. Alloys Compd. **282**, 79 (1999).
[31] D. Hautot and G. J. Long (unpublished).